Nonlinear-dynamical arrhythmia control in humans

David J. Christini†, Kenneth M. Stein, Steven M. Markowitz, Suneet Mittal, David J. Slotwiner, Marc A. Scheiner, Sei Iwai, and Bruce B. Lerman

Department of Medicine, Division of Cardiology, Cornell University Medical College, New York, NY 10021

Edited by Charles S. Peskin, New York University, New York, NY, and approved February 28, 2001 (received for review November 21, 2000)

Nonlinear-dynamical control techniques, also known as chaos control, have been used with great success to control a wide range of physical systems. Such techniques have been used to control the behavior of *in vitro* excitable biological tissue, suggesting their potential for clinical utility. However, the feasibility of using such techniques to control physiological processes has not been demonstrated in humans. Here we show that nonlinear-dynamical control can modulate human cardiac electrophysiological dynamics by rapidly stabilizing an unstable target rhythm. Specifically, in 52/54 control attempts in five patients, we successfully terminated pacing-induced period-2 atrioventricular-nodal conduction alternans by stabilizing the underlying unstable steady-state conduction. This proof-of-concept demonstration shows that nonlinear-dynamical control techniques are clinically feasible and provides a foundation for developing such techniques for more complex forms of clinical arrhythmia.

Increasingly, it is recognized that many cardiac arrhythmias can be characterized on the basis of the physical principles of nonlinear dynamics (1, 2). A nonlinear-dynamical system is one that changes with time and cannot be broken down into a linear sum of its individual components. For certain nonlinear systems, known as chaotic systems, behavior is aperiodic and long-term prediction is impossible, even though the dynamics are entirely deterministic (i.e., the dynamics of the system are completely determined from known inputs and the previous state of the system, with no influence from random inputs). Importantly, such determinism actually can be exploited to control the dynamics of a chaotic system. To this end, a variety of nonlinear-dynamical control techniques, also known as chaos control,‡ have been developed (3, 4) and applied successfully to a wide range of physical systems (5–14). Such techniques are model-independent, i.e., they require no *a priori* knowledge of the underlying equations of a system and are therefore appropriate for systems that are essentially ''black boxes.''

The success of nonlinear-dynamical control techniques in stabilizing physical systems, together with the facts that many physiological systems are nonlinear (e.g., the cardiac conduction system, because of its numerous complex nonlinear component interactions) and lack the detailed analytical system models required for model-based control techniques, have fostered widespread interest in applying these model-independent techniques to biological dynamical systems (15–26). In a pioneering application, Garfinkel *et al.* (15) stabilized drug-induced irregular cardiac rhythms by means of dynamically timed electrical stimulation in an *in vitro* rabbit ventricular-tissue preparation. That work was an important demonstration that the physical principles of nonlinear-dynamical control could be extended into the realm of cardiac dynamics. Although extension of that work to the control of fibrillation in intact hearts is impeded currently by the complexity of fibrillation [notwithstanding a recent study that showed interesting dynamical modification of human atrial fibrillation (27)], there are clinically important low-dimensional cardiac dynamics (e.g., reentrant arrhythmias) for which such techniques are well suited. Control of such dynamics has been demonstrated in computational studies of mathematical arrhythmia models (19, 21) and in *in vitro* rabbit heart experiments (22). In this study, we demonstrate that such dynamics also can be controlled in humans.

Methods

Background. To demonstrate clinical feasibility, we have attempted to control a dynamically tractable rhythm known as atrioventricular (AV) nodal conduction alternans (referred to hereafter as alternans). Alternans is a beat-to-beat alternation in AV-nodal conduction time that can develop if the time between consecutive AV-nodal excitations is abnormally short—the AV-nodal conduction time gradually fatigues (lengthens) and then bifurcates from its steady-state value into an alternation; such a bifurcation is a hallmark of a nonlinear-dynamical system. AV-nodal alternans is not clinically dangerous. However, alternans is of interest to nonlinear dynamicists, because it is a clinically inducible cardiac rhythm that can be used to study how nonlinear-dynamical control methods can exploit arrhythmia dynamics for arrhythmia termination. Furthermore, as will be discussed later, the underlying dynamics of alternans may be related to more dangerous cardiac dynamics.

Clinically, alternans often has been attributed to the presence of dual AV-nodal pathways (28). However, Billette and coworkers (29, 30) have demonstrated clearly that alternans can result solely from the conduction properties of a single AV-nodal pathway. In fact, alternans attributed to a single AV-nodal pathway have been observed in humans during AV orthodromic reciprocating tachycardia (ORT; refs. 31 and 32), a repetitive reentrant arrhythmia in which normal anterograde ventricular excitation by means of the AV node is followed by reexcitation of the atria by means of a pathological retrograde accessory ventriculoatrial pathway.

Technique. An alternans pacing and control protocol was performed, after informed written consent was obtained, as a supplementary component of routine clinically indicated electrophysiological studies in five patients (3 males, 2 females; 52 ±17 yr) with normal AV-nodal conduction (see Table 1 for patient demographics and control-algorithm results). In two patients, trials were performed preceding and after pharmacological autonomic blockade, which was administered by means of i.v. delivery of 0.2 mg/kg propranolol and 0.04 mg/kg atropine (33). The pharmacological blockade trials were used to ensure that control-algorithm results were not related to autonomic influences on AV-nodal function. In two other patients, because alternans did not occur in the absence of pharmacological autonomic blockade, the control protocol was performed only after blockade. In one patient, alternans did occur in the absence of pharmacological autonomic blockade but a second trial after blockade was not performed, because β-blockade was contraindicated due to the patient's underlying chronic obstructive pulmonary disease.

The electrophysiological studies used standardized techniques

This paper was submitted directly (Track II) to the PNAS office.

Abbreviations: AV, avioventricluar; ORT, orthodromic reciprocating tachycardia; VA, ventriculoatrial; AH, atrial-His.

†To whom reprint requests should be addressed at: Cornell University Medical College, 520 East 70th Street, Starr-463, New York, NY 10021. E-mail: dchristi@med.cornell.edu.

‡Note that in this paper, ''control'' refers to a method of altering dynamics, not a standard comparative group for an experiment.

The publication costs of this article were defrayed in part by page charge payment. This article must therefore be hereby marked "*advertisement*" in accordance with 18 U.S.C. §1734 solely to indicate this fact.

Table 1. Demographics and control-trial results

Subject	Age/sex	Dual AV-nodal pathways?	Antiarrhythmic medications	Heart disease	Electrophysiology study indication	Pre/post autonomic blockade	Control successes/attempts	Different nominal VAs	$\bar{\sigma}_p$, ms	$\bar{\sigma}_c$, ms	Δ_σ, %
1	38/F	Yes	None	WPW	Palpitations, presyncope	Post	14/14	9	17.3	6.1	65
2	35/F	No	None	WPW	SVT	Pre	8/8	4	14.1	9.0	36
2	35/F	No	None	WPW	SVT	Post	8/8	4	12.0	3.9	68
3	62/M	Yes	Digoxin, disopyramide	—	SVT	Pre	2/2	2	43.8	28.5	35
3	62/M	Yes	Digoxin, disopyramide	—	SVT	Post	2/2	1	5.4	3.1	43
4	75/M	No	Digoxin, verapamil	CAD, HTN	SVT	Pre	10/10	3	9.7	4.3	56
5	51/M	No	Digoxin	IDCM	SVT	Post	8/10	1	9.1	5.0	45

$\bar{\sigma}_p$, $\bar{\sigma}_c$, and Δ_σ are defined in *Results.* WPW, Wolf–Parkinson–White syndrome; CAD, coronary artery disease; HTN, hypertension; IDCM, idiopathic dilated cardiomyopathy; SVT, supraventricular tachycardia.

that included the introduction of multiple percutaneous catheters from the femoral veins to record intracardiac signals from the right atrium, the His bundle region, and the right ventricle, as well as to pace from the two chambers. In studies in which isoproterenol was delivered during the clinical evaluation stage, the alternans pacing and control protocol was not initiated until at least 15 min after the termination of isoproterenol delivery.

During each trial, ORT was simulated by means of a protocol called fixed-delay stimulation (Fig. 1), in which the right atrium was stimulated (at time *A*) at a fixed time interval, VA (ventriculoatrial), after detection of ventricular activation (at time *V*). When the VA interval is reduced (simulating faster reentry), the approximately (i.e., there is a small degree of inherent conduction variability) period-1 rhythm can destabilize and the AV-nodal conduction time can bifurcate into period-2 alternans. Note that in this study, rhythms more complex than alternans were not observed; however, in a larger clinical study of AV-nodal conduction dynamics during rapid atrial pacing, more complex AV-nodal rhythms, including period-4 conduction, were seen (34).

A surface electrogram was sampled at 1 kHz by a National Instruments (Austin, Texas) AT-MIO-16E-10 data acquisition board in a 266-MHz Intel Pentium-II-powered computer running Real-Time Linux and a custom C++ experiment interface system (35). To simulate ORT, this system automatically detected R-waves in the surface electrogram (denoted time *V*) by means of a threshold-crossing algorithm and then, at a predetermined VA interval after the detected R-wave, output a voltage pulse by means of the AT-MIO-16E-10 to trigger a Bloom DTU215 stimulator (Fischer Imaging, Denver) to stimulate the right atrium (at time *A*; Fig. 1). The nominal VA interval was decreased gradually until an alternation (alternans) in the AV interval was observed.

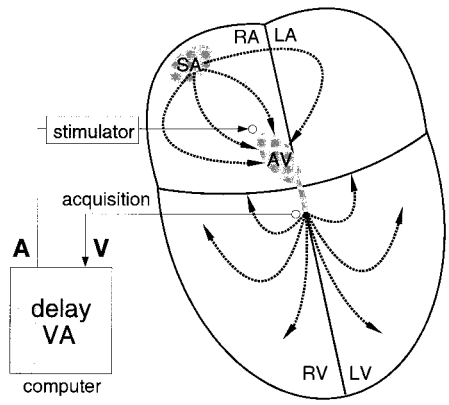

Fig. 1. A schematic showing normal conduction from the sinoatrial (SA) node, through the right and left atria (RA, LA), the AV node, and the right and left ventricles (RV, LV). In the absence of an abnormal retrograde pathway, ORT can be simulated (as depicted by the loop containing the computer) by fixed-delay stimulation of the right atrium (at time *A*) at an interval, VA, after detection of ventricular activation (at time *V*).

Once alternans occurred, an adaptive nonlinear-dynamical control technique (36) was initiated to terminate the alternans. The control algorithm is designed to stabilize the underlying unstable steady state, x^*, of a system that can be described by a unimodal one-dimensional function ($x_{n+1} = f(x_n, p_n)$, where x_n is the current value of the system variable of interest, x (for alternans, x is the AV-nodal conduction time, AV), x_{n+1} is the next value of the same variable, and p_n is the current value of an accessible system parameter p (for alternans control, p is the VA-pacing interval) at index n. Thus, for alternans, the system function is

$$\mathrm{AV}_{n+1} = f(\mathrm{AV}_n, \mathrm{VA}_n), \qquad [1]$$

where n is the beat number. The control technique perturbs VA such that

$$\mathrm{VA}_n = \overline{\mathrm{VA}} + \delta\mathrm{VA}_n, \qquad [2]$$

where $\overline{\mathrm{VA}}$ is the nominal VA-pacing interval, and $\delta\mathrm{VA}_n$ is a perturbation (6, 7, 37) given by

$$\delta\mathrm{VA}_n = \frac{\mathrm{AV}_n - \mathrm{AV}_n^*}{g_n}, \qquad [3]$$

where AV_n^* is the current estimate of the unstable steady state AV*, and g_n is the control sensitivity g at index n. Thus, for each atrial stimulus, the nonlinear-dynamical control algorithm computes a perturbation to the nominal VA interval that is proportional to the difference between the current AV interval and the targeted unstable period-1 AV steady state.

Importantly, only negative perturbations (i.e., those that result in a shortening of the VA interval) are permitted. If the perturbation computed for a given VA interval is positive, the nominal VA interval is left unperturbed. This condition is imposed to simulate the ability of a pacemaker to truncate but not lengthen VA during a hypothetical episode of clinical ORT (i.e., the natural ORT impulse would excite the AV node before any stimulus attempted at a lengthened VA interval).

The dynamics of alternans and control are depicted schematically in Fig. 2. In Fig. 2, $f(\mathrm{AV}_n, \overline{\mathrm{VA}})$ is represented by a quadratic curve fit to uncontrolled AV intervals that obeyed the dynamics of Eq. **1**. During stable alternans (i.e., without control) (Fig. 2*a*), the AV intervals alternate indefinitely between points 1 and 2 via the dynamic route depicted by the dotted lines, and never move into the unstable interior region of the function. With control (Fig. 2*b*), the appropriate $\overline{\mathrm{VA}}$ control perturbation of Eq. **3** shifts the function to $f(\mathrm{AV}_n, \overline{\mathrm{VA}} + \delta\mathrm{VA}_n)$. By doing so, point 1 becomes point 1′ (i.e., AV_{n+1} is increased). When the function

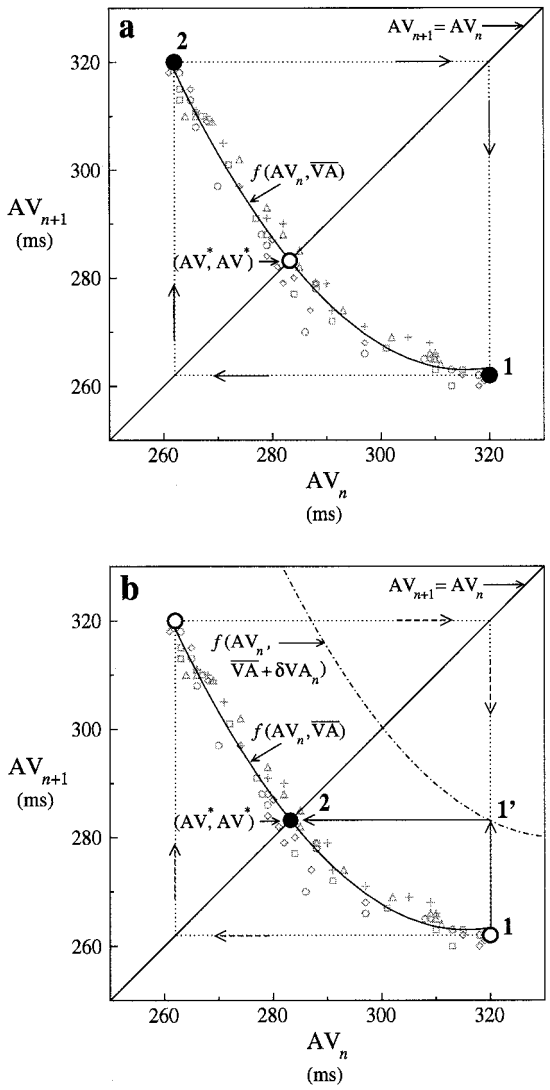

Fig. 2. A schematic of AV interval dynamics without (*a*) and with (*b*) control. In both panels the schematic is superimposed over five series of AV intervals (annotated with different gray symbols) that correspond to consecutive control attempts at the same nominal VA interval in one alternans pacing and control trial. These AV intervals immediately followed control termination, and therefore obeyed $f(AV_n, \overline{VA})$ as they drifted away from the unstable steady state AV* and back into alternans. Thus, $f(AV_n, \overline{VA})$ was approximated by a quadratic curve fit to the AV intervals. The intersection of $f(AV_n, \overline{VA})$ with the line of identity (the diagonal line $AV_{n+1} = AV_n$) is the unstable steady state AV*. Without control (*a*), the AV intervals alternate indefinitely between points 1 and 2 via the dynamic route depicted by the dotted lines, and never explore the unstable interior region of $f(AV_n, \overline{VA})$. *b* shows how the VA control perturbation of Eq. **3** shifts the function along the line of identity to the location of the dash-dot curve $f(AV_n, \overline{VA} + \delta VA_n)$. By doing so, point 1 becomes point 1′ (i.e., AV_{n+1} is increased). When the function is returned to $f(AV_n, \overline{VA})$ at the next beat (i.e., $\delta VA_{n+1} = 0$), control succeeds as the AV interval progresses to point 2, which is at the unstable steady state AV*.

is returned to $f(AV_n, \overline{VA})$ at the next beat (i.e., $\delta VA = 0$), AV progresses to point 2—the unstable period-1 steady state AV*. Repetition of such perturbations, always calculated according to the current system state, holds the system within the neighborhood of AV*. Termination of control would be followed by the drift of AV away from AV*, through the unstable interior region, back to the stable alternans rhythm of Fig. 2*a*.

Both AV* and *g* are estimated adaptively at each beat, thereby providing inherent algorithmic dynamic flexibility. For alternans, AV_n^* is reestimated repeatedly as the midpoint of AV_n and AV_{n-1}.[§] The control sensitivity *g* is adapted in real time based on the characteristic dynamics of unimodal one-dimensional systems. Specifically, for every beat, if the sign of the computed perturbation (Eq. **3**) has alternated for the four previous perturbations, the magnitude of *g* is decreased by a factor ρ (for this study $\rho = 0.05$), otherwise, the magnitude of *g* is increased by a factor ρ (36).

Importantly, this nonlinear-dynamical control technique estimates the control parameters and target-rhythm dynamics in real time "on-the-fly" (i.e., requiring no learning stage). This feature has two significant benefits, especially for clinical applications. First, the repetitive estimation provides inherent robustness to nonstationarities, because any change in the underlying system dynamics will be immediately detected and accounted for. Second, the instantaneous onset of parameter estimation eliminates the need for a precontrol learning stage (3), which is a period often required before control activation to quantify the system dynamics. With this on-the-fly approach, the algorithm learns the dynamics at the same time that it is bringing the system under control. Thus, it is capable of applying control immediately on the detection of an arrhythmia (avoiding dangerous lag time) and is able to maintain control as the dynamics of the arrhythmia change over time.

Results

The alternans pacing and control algorithm results for the five patients are shown in Table 1. Control was successful in 52 of 54 control attempts (96%). To quantify control-stage efficacy, the standard deviation of the 15 AV intervals immediately preceding each control stage [(σ_{p_k}), where *k* is the index of a given control stage)] and the standard deviation of the AV intervals during each control stage (σ_{c_k}) were calculated. From these values, the mean precontrol standard deviation ($\overline{\sigma_p} = \frac{1}{N}\Sigma_{k=1}^{N}\sigma_{p_k}$, where *N* is the total number of control stages for the trial) and the mean control-stage standard deviation ($\overline{\sigma_c} = \frac{1}{B}\Sigma_{k=1}^{N} b_k\sigma_{c_k}$, where b_k is the number of beats for the *k*th control stage and $B = \Sigma_{k=1}^{N} b_k$) were computed. The control improvement was quantified as the percentage of the precontrol AV-interval standard deviation eliminated during control: $\Delta_\sigma = 100(1 - \overline{\sigma_c}/\overline{\sigma_p})$. Control improvement ranged from 35% to 68%. Control efficacy was independent of the presence of dual AV-nodal pathways [dual-pathway physiology was tested without pharmacological autonomic blockade; trials on patients with dual pathways: 48 ± 16% (Δ_σ mean ± standard deviation); and without dual pathways: 51 ± 14%, *P* = not significant (NS)], antiarrhythmic medications (trials on patients taking antiarrhythmic medications: 45 ± 9%; and not taking antiarrhythmic medications: 56 ± 18%, *P* = NS), or autonomic blockade (trials before autonomic blockade: 42 ± 12%; and after autonomic blockade: 55 ± 13%, *P* = NS).

Fig. 3 shows a representative example of a patient undergoing simulated ORT pacing after propranolol/atropine autonomic blockade (Patient 1). Before the initiation of control, the fixed VA-pacing interval of 60 ms caused an alternation in the atrial-His (AH) interval between 127 and 167 ms.[¶] On control initiation, the VA nonlinear-dynamical control perturbations (Eq. **3**) moved the AH intervals toward their underlying steady state, which lies between the bifurcated alternating values.

Fig. 4 shows the time course of a segment of the trial shown in Fig. 3. The control perturbations made to the VA interval (Fig. 4*b*) terminated the alternating AV-nodal conduction by forcing

[§]For higher-order rhythms, additional previous values of the system variable may be incorporated into the estimate (40).

[¶]Note that the AH interval, which is the AV-nodal conduction time, is quantifiable during posttrial analysis of electrograms. Because reliable His-bundle detection is not possible during a control trial, the AV interval is used as a surrogate for the AH interval. This substitution is based on the assumption that the HV interval is fixed, an assumption that was verified for each patient during atrial pacing at multiple cycle lengths.

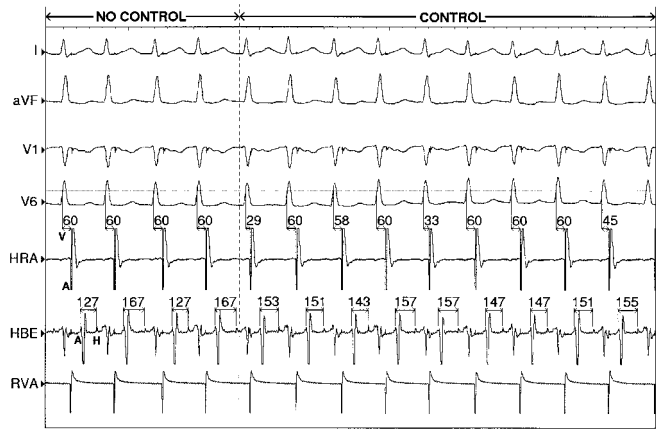

Fig. 3. Surface (leads I, aVF, V1, and V6) and intracardiac (HRA, high right atrium; HBE, His bundle; and RVA, right ventricular apex) electrograms from a segment of an alternans control trial (Patient 1). The two rows of numeric annotations mark the VA (upper) and AH (lower) intervals in ms. Note that the onset of atrial activity (A) in HBE occurs later than in HRA, reflecting intraatrial conduction time. The VA intervals are measured as the time between the electrogram threshold (represented by the dotted horizontal line superimposed over V6) crossing and the stimulus delivery. Before control initiation (i.e., to the left of the vertical dashed line), VA was held fixed at 60 ms, corresponding to AH alternans between 127 and 167 ms. After control was initiated, VA nonlinear-dynamical control perturbations resulted in termination of alternans as the AH interval was moved into the neighborhood of its underlying unstable steady state. As a result of the biological requirement that $\delta VA_n < 0$ (Eq. 3), a negative perturbation was delivered (i.e., VA < 60 ms) every second to fourth beat. This electrogram corresponds to beats 1,287 to 1,299 in Fig. 4.

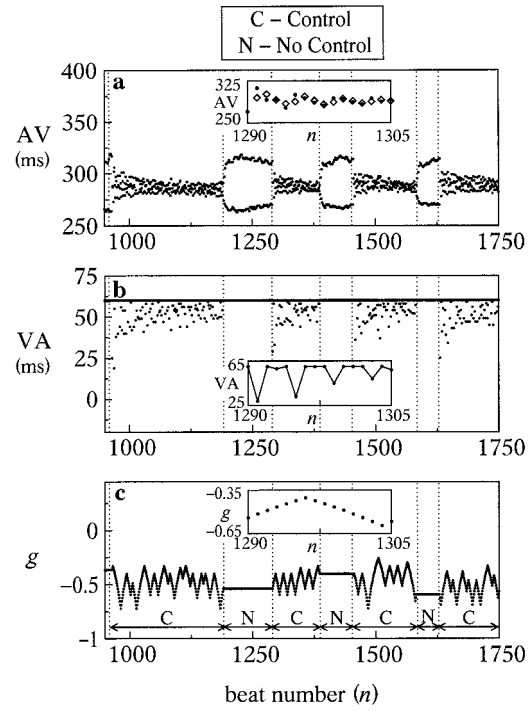

Fig. 4. A segment of an alternans control trial (Patient 1). *a*, *b*, and *c* show AV, VA, and *g* vs. beat number *n* for various stages (as annotated in *c*) of the control trial. VA nonlinear-dynamical control perturbations terminated the alternans in each of the control attempts. The *Insets* in each panel show the first 15 beats of the second control attempt ($1{,}290 \leq n \leq 1{,}305$). During this time, the adaptive flexibility of the algorithm is apparent by means of the algorithmic modifications made to the AV steady-state estimate [*a Inset*, AV (filled circles) and AV steady-state estimate (open diamonds)] and to *g* (*c Inset*). The changes in *g* were dictated (as described in *Methods* and ref. 36) by every second beat ($1{,}290 \leq n \leq 1{,}295$) to every fourth beat ($1{,}296 \leq n \leq 1{,}303$) and back to every second beat ($1{,}303 \leq n \leq 1{,}305$) VA perturbation patterns (*b Inset*).

the AV interval toward its underlying unstable steady state (Fig. 4*a*). Tight, noise-free control was not possible because of the biological noise inherent to this system.

Importantly, on termination of each control stage, the AV interval reverted spontaneously to alternans. This spontaneous reversion demonstrates that the steady state was unstable, that the nonlinear-dynamical control perturbations were required for stabilization, and that the alternans termination was not a coincidental spontaneous occurrence. An alternative hypothesis, that control resulted from a reversion to single-pathway conduction from dual-pathway alternation, is refuted by the fact that period-1 conduction was at an interval between the two alternating conduction intervals rather than at one rate or the other. The single-pathway hypothesis is further supported by (*i*) the fact that the onset of alternans was characterized by a bifurcation (typical of nonlinear-dynamical function) instead of a discrete jump (typical of dual-pathway function) and (*ii*) successful control in three patients who did not have dual AV-nodal pathways.

The adaptive control algorithm's inherent ability to track nonstationarities was demonstrated later in the same trial, as shown in Fig. 5. During each control attempt, the nominal VA interval, $\overline{VA}$, was increased or decreased in discrete steps. For example, Fig. 5*b* shows that from $2{,}900 \leq n \leq 3{,}115$, $\overline{VA}$ was increased from 15 to 55 ms. During this time, the control algorithm never lost its AV stabilization, even as its unstable steady state shifted from 320 to 285 ms (Fig. 5*a*).

For Patient 1, nonlinear-dynamical control was applied 14 distinct times; each control attempt successfully eliminated the alternans rhythm ($\overline{\sigma_p}$ = 17.3 ms, $\overline{\sigma_c}$ = 6.1 ms, and Δ_σ = 65%). In Patient 2, control was attempted in two trials, one before and one after propranolol/atropine autonomic blockade. In the preblockade trial, control was attempted 8 times at four different nominal VA intervals and was successful each time ($\overline{\sigma_p}$ = 14.1 ms, $\overline{\sigma_c}$ = 9.0 ms, and Δ_σ = 36%). In the postblockade trial, control was attempted 8 times at four different nominal VA intervals and was successful each time ($\overline{\sigma_p}$ = 12.0 ms, $\overline{\sigma_c}$ = 3.9 ms, and Δ_σ = 68%). In Patient 3, control also was attempted before and after propranolol/atropine autonomic blockade. In the preblockade trial, control was attempted twice at two different nominal VA intervals and was successful both times ($\overline{\sigma_p}$ = 43.8 ms, $\overline{\sigma_c}$ = 28.5 ms, and Δ_σ = 35%). In the postblockade trial, control was attempted twice at one VA interval and was successful both times ($\overline{\sigma_p}$ = 5.4 ms, $\overline{\sigma_c}$ = 3.1 ms, and (Δ_σ = 43%). (Most alternans occurrences for this patient were transient and therefore inappropriate for control attempts.) In Patient 4, control was attempted without autonomic blockade 10 times at three different nominal VA intervals and was successful each time ($\overline{\sigma_p}$ = 9.7 ms, $\overline{\sigma_c}$ = 4.3 ms, and Δ_σ = 56%). In Patient 5, control was successful in 8 of 10 attempts at a single nominal VA interval after propranolol/atropine autonomic blockade ($\overline{\sigma_P}$ = 9.1 ms, $\overline{\sigma_c}$ = 5.0 ms, and Δ_σ = 45%; values were computed by using only successful control stages). The two control failures seemed to result from the fact that $\overline{VA}$ = 10 ms, which left little room for VA interval shortening, thereby increasing the difficulty of unstable steady-state capture. The AV and VA intervals and *g* proportionality constant for Patients 2–5 were all qualitatively similar to those shown in Fig. 4.

Discussion

In this study, we have demonstrated that nonlinear-dynamical control techniques can be used effectively in humans. We have shown, in 52/54 control attempts in five patients, that an adaptive

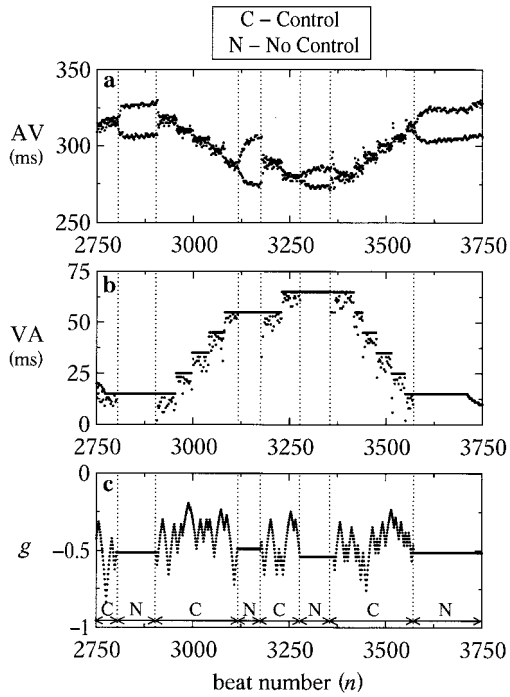

Fig. 5. Control of nonstationary alternans (Patient 1). *a*, *b*, and *c* show AV, VA, and *g* vs. beat number *n* for various stages (as annotated in *c*) of the control trial. During each control stage, the nominal VA interval was either increased or decreased (as seen in *b*), causing a corresponding drift in the underlying period-1 AV steady state. Nevertheless, nonlinear-dynamical control perturbations made to VA maintained control of AV as it moved through the different parameter regimes.

on-the-fly (i.e., requiring no learning stage) nonlinear-dynamical control technique can alter cardiac dynamics by simultaneously estimating and stabilizing an unstable target rhythm. Control efficacy was not related to antiarrhythmic medications, the presence of dual AV-nodal pathways, or autonomic influences (i.e., control was effective both with and without pharmacological autonomic blockade). These findings provide support for earlier suggestions that nonlinear-dynamical control might be applicable to clinical arrhythmia control (1, 2, 15, 19, 22).

Nonlinear-Dynamical Control. The idea of using the dynamics of a chaotic system for system control was proposed in the early 1990s by Ott *et al.* (3). Their approach took advantage of the fact that the aperiodic dynamics of a chaotic system are actually composed of an infinite number of unstable steady-state rhythms. Chaotic aperiodicity stems from the inability of a chaotic system to remain in any one of its repellent unstable periodic rhythms. The Ott *et al.* technique attempts to regularize the dynamics of a chaotic system by holding it within a targeted unstable rhythm by exploiting the characteristic dynamics of that rhythm. Such control is possible because, although long-term forecasting of a chaotic system is impossible, short-term dynamical prediction is possible. Furthermore, such short-term prediction can be extended to account for and exploit the effects of a perturbed system parameter. With such dynamical knowledge, a corrective parameter perturbation can be used to move the system into, and hold it within, the neighborhood of a desired unstable steady-state rhythm.

Importantly, the Ott *et al.* (3) technique is model-independent, i.e., it requires no *a priori* knowledge of the underlying equations of a system. Model-independent techniques extract necessary quantitative information (about the functional dependence of the variable to be controlled on a system parameter) from system observations and then use this information to exploit the inherent dynamics of the system to achieve a desired control result. Thus, these techniques are applicable to systems for which analytical models are typically unavailable or incomplete, i.e., "black boxes."

The Ott *et al.* (3) technique, and its derivatives, have been applied to control a wide range of physical systems (3, 4) including magneto-elastic ribbons (5), electronic circuits (6, 10, 11), lasers (8, 12), chemical reactions (7, 9), and driven pendulums (13, 14). The success of nonlinear-dynamical control in stabilizing physical systems has fostered interest in applying these techniques to excitable biological systems (15–19, 21, 22). It is the model-independent nature of such techniques that make them particularly well suited for biological systems—although many physiological mechanisms are well understood qualitatively, quantitative relationships between physiological system components are usually incomplete. Thus, because accurate analytical system models cannot be developed for such systems, model-based control techniques are often not applicable to physiological systems. In contrast, model-independent techniques are applicable because, before control, they require only a qualitative understanding of the underlying dynamical mechanisms.

Nonlinear-Dynamical Control of Cardiac Dynamics. In a pioneering biological nonlinear-dynamical control application, Garfinkel *et al.* (15) stabilized drug-induced irregular cardiac rhythms in tissue from the interventricular septum of a rabbit heart. They applied electrical nonlinear-dynamical control perturbations directly to the interbeat intervals to hold the system within an underlying unstable steady state. They successfully regularized the electrical activity into low-order rhythms, but not the period-1 rhythm they targeted. Subsequent mathematical modeling studies have suggested dynamical mechanisms for such control-algorithm results, along with improved adaptive algorithms that could achieve "tighter" control (39–42).

The provocative cardiac chaos-control study by Garfinkel *et al.* (15), combined with data suggesting that fibrillation is chaotic (43, 44), sparked interest in nonlinear-dynamical control of fibrillation. However, other work has questioned the chaotic fibrillation hypothesis (45, 46). The current prevailing theory (47), supported by a range of mathematical (48–56), *in vitro* (57–59), and *in vivo* (57, 60–70) studies, is that fibrillation is a complex nonlinear combination of stochastic and deterministic components, such as scroll waves of electrical activity meandering within the ventricular wall. Given this body of evidence, it is apparent that fibrillation is characterized by high-dimensional nonstationary spatiotemporal dynamics that are too complex for current nonlinear-dynamical control techniques.

Nevertheless, nonlinear-dynamical control is still applicable to the control of cardiac arrhythmias because, as with chaotic systems, nonlinear-dynamical systems with regular dynamics may have underlying unstable steady states. Such steady states can be targeted for rhythm control by using derivatives of the Ott *et al.* (3) technique (71). This approach has been demonstrated in mathematical modeling of cardiac dynamics (19, 21) and *in vitro* rabbit heart studies (22).

Nonlinear-Dynamical Control of Clinical Cardiac Dynamics. In this study, we now have demonstrated the utility of such techniques in humans. These results suggest that nonlinear-dynamical control could be used for clinical arrhythmia control. In particular, nonlinear-dynamical suppression of cardiac alternans may have important clinical implications given that alternans in electrocardiogram morphology, such as T-wave alternans, can precede life-threatening arrhythmias and is a risk factor for sudden death (72–76). T-wave alternans is the surface electrocardiographic marker of a beat-to-beat alternation in ventricular repolarization. The period-2 nature of T-wave alternans suggests that, like AV-nodal alternans, it may be amenable to nonlinear-dynamical control techniques. However, because T-wave alternans is distributed spatially over the surface of

the ventricles (unlike the spatially localized AV-nodal alternans controlled in this study), nonlinear-dynamical methods applied to it must be capable of spatiotemporal control (25, 26, 77–81). If such control is successful, a potential route to a sustained ventricular arrhythmia may be eliminated (72–76) thereby preventing the onset of a potentially deadly arrhythmic event.

More generally, the flexibility and adaptability of nonlinear-dynamical control techniques may improve ventricular tachycardia therapies. Antitachycardia pacing algorithms used in current-generation implantable cardiac defibrillators do not use beat-to-beat feedback information during stimulation. In contrast, adaptive nonlinear-dynamical control techniques alter their intervention parameters, such as interstimulus interval, on a beat-to-beat basis according to the effects of previous stimuli on the dynamics of the arrhythmia. By doing so, such "smart" algorithms exploit the underlying dynamics of the arrhythmia they are attempting to terminate—essentially using the dynamics of the arrhythmia against the arrhythmia itself. In summary, nonlinear-dynamical control techniques, by means of their inherent adeptness at characterizing and exploiting the underlying nonlinear nature of arrhythmias, have the potential to provide novel approaches to the treatment of clinical arrhythmias.

Limitations. Although the findings of this study suggest the feasibility of nonlinear-dynamical control of cardiac arrhythmias in general, the applicability of this particular control algorithm to arrhythmias other than induced AV-nodal alternans is unclear, given that the alternans termination in this study corresponds to a modification of AV-nodal conduction (not actual termination of conduction) that is qualitatively different from the termination (not modification) of a reentrant wave. Another limitation of this study was that control efficacy was restricted by the 1-ms stimulus-timing resolution of the stimulator. Because unstable steady states are highly sensitive to small parameter deviations, it is possible that a finer stimulus-timing resolution could result in tighter rhythm control. An additional limitation was the need for visual alternans recognition and the corresponding manual activation (by means of a software toggle switch) of the nonlinear-dynamical control algorithm. In an arrhythmia-control device, arrhythmia recognition and control activation would have to be automated.

This work was supported, in part, by grants from the American Heart Association (National Center no. 0030028N and New York City Affiliate no. 9950993T), the Raymond and Beverly Sackler Foundation, and the National Institutes of Health Grant R01 HL-56139.

1. Glass, L. (1996) *Phys. Today* **49** (8), 40–45.
2. Christini, D. J., Stein, K. M., Markowitz, S. M., Mittal, S., Slotwiner, D. J. & Lerman, B. B. (1999) *Heart Dis.* **1,** 190–200.
3. Ott, E., Grebogi, C. & Yorke, J. A. (1990) *Phys. Rev. Lett.* **64,** 1196–1199.
4. Lindner, J. F. & Ditto, W. L. (1995) *Appl. Mech. Rev.* **48,** 795–808.
5. Ditto, W. L., Rauseo, S. N. & Spano, M. L. (1990) *Phys. Rev. Lett.* **65,** 3211–3214.
6. Hunt, E. R. (1991) *Phys. Rev. Lett.* **67,** 1953–1955.
7. Peng, B., Petrov, V. & Showalter, K. (1991) *J. Phys. Chem.* **95,** 4957–4959.
8. Roy, R., Murphy, Jr., T. W., Maier, T. D., Gills, Z. & Hunt, E. R. (1992) *Phys. Rev. Lett.* **68,** 1259–1262.
9. Petrov, V., Gáspár, V., Masere, J. & Showalter, K. (1993) *Nature (London)* **361,** 240–243.
10. Gauthier, D. J., Sukow, D. W., Concannon, H. M. & Socolar, J. E. S. (1994) *Phys. Rev. E Stat. Phys. Plasmas Fluids Relat. Interdiscip. Top.* **50,** 2343–2346.
11. Socolar, J. E. S., Sukow, D. W. & Gauthier, D. J. (1994) *Phys. Rev. E Stat. Phys. Plasmas Fluids Relat. Interdiscip. Top.* **50,** 3245–3248.
12. Colet, P., Roy, R. & Wiesenfeld, K. (1994) *Phys. Rev. E Stat. Phys. Plasmas Fluids Relat. Interdiscip. Top.* **50,** 3453–3457.
13. Hübinger, B., Doerner, R., Martienssen, W., Herdering, M., Pitka, R. & Dressler, U. (1994) *Phys. Rev. E Stat. Phys. Plasmas Fluids Relat. Interdiscip. Top.* **50,** 932–948.
14. Christini, D. J., Collins, J. J. & Linsay, P. S. (1996) *Phys. Rev. E Stat. Phys. Plasmas Fluids Relat. Interdiscip. Top.* **54,** 4824–4827.
15. Garfinkel, A., Spano, M. L., Ditto, W. L. & Weiss, J. N. (1992) *Science* **257,** 1230–1235.
16. Schiff, S. J., Jerger, K., Duong, D. H., Chang, T., Spano, M. L. & Ditto, W. L. (1994) *Nature (London)* **370,** 615–620.
17. Christini, D. J. & Collins, J. J. (1995) *Phys. Rev. Lett.* **75,** 2782–2785.
18. Watanabe, M. & Gilmour, R. F. (1996) *J. Math. Biol.* **35,** 73–87.
19. Christini, D. J. & Collins, J. J. (1996) *Phys. Rev. E Stat. Phys. Plasmas Fluids Relat. Interdiscip. Top.* **53,** R49–R52.
20. Brandt, M. E. & Chen, G. (1996) *Int. J. Bifurc. Chaos* **6,** 715–723.
21. Brandt, M. E., Shih, H.-T. & Chen, G. (1997) *Phys. Rev. E Stat. Phys. Plasmas Fluids Relat. Interdiscip. Top.* **56,** R1334–R1337.
22. Hall, K., Christini, D. J., Tremblay, M., Collins, J. J., Glass, L. & Billette, J. (1997) *Phys. Rev. Lett.* **78,** 4518–4521.
23. Biktashev, V. N. & Holden, A. V. (1994) *J. Theor. Biol.* **169,** 101–112.
24. Biktashev, V. N. & Holden, A. V. (1995) *Proc. R. Soc. London Ser. B* **260,** 211–217.
25. Mantel, R.-M. & Barkley, D. (1996) *Phys. Rev. E Stat. Phys. Plasmas Fluids Relat. Interdiscip. Top.* **54,** 4791–4801.
26. Biktashev, V. N. & Holden, A. V. (1998) *Chaos* **8,** 48–56.
27. Ditto, W. L., Spano, M. L., In, V., Neff, J., Meadows, B., Langberg, J. J., Bolmann, A. & McTeague, K. (2000) *Int. J. Bifurc. Chaos* **10,** 593–601.
28. Sung, R. J. & Styperek, J. L. (1979) *Circulation* **60,** 1464–1476.
29. Sun, J., Amellal, F., Glass, L. & Billette, J. (1995) *J. Theor. Biol.* **173,** 79–91.
30. Amellal, F., Hall, K., Glass, L. & Billette, J. (1996) *J. Cardiovasc. Electrophysiol.* **7,** 943–951.
31. Krikler, D. & Rowland, E. (1979) in *Cardiac Arrhythmias: Electrophysiology, Diagnosis, and Management*, ed. Narula, O. (Williams & Wilkins, Baltimore), pp. 382–396.
32. Rinkenberger, R. L., Prystowsky, E. N., Heger, J. J., Troup, P. J., Jackman, W. M. & Zipes, D. P. (1980) *Circulation* **62,** 996–1010.
33. Jose, A. D. & Taylor, R. R. (1969) *J. Clin. Invest.* **48,** 2019–2031.
34. Christini, D. J., Stein, K. M., Markowitz, S. M., Mittal, S., Slotwiner, D. J., Iwai, S. & Lerman, B. B. *Am. J. Physiol.*, in press.
35. Christini, D. J., Stein, K. M., Markowitz, S. M. & Lerman, B. B. (1999) *Ann. Biomed. Eng.* **27,** 180–186.
36. Hall, K. & Christini, D. J. (2001) *Phys. Rev. E Stat. Phys. Plasmas Fluids Relat. Interdiscip. Top.* **63,** article 046204.
37. Petrov, V., Peng, B. & Showalter, K. (1992) *J. Chem. Phys.* **96,** 7506–7513.
38. Christini, D. J. & Collins, J. J. (1997) *IEEE Trans. Circuits Syst. I* **44,** 1027–1030.
39. Glass, L. & Zeng, W. (1994) *Int. J. Bifurc. Chaos* **4,** 1061–1067.
40. Christini, D. J. & Collins, J. J. (1997) *Chaos* **7,** 544–549.
41. Sauer, T. (1997) *Fields Institute Communication* **11,** 63–75.
42. Christini, D. J. & Kaplan, D. T. (2000) *Phys. Rev. E Stat. Phys. Plasmas Fluids Relat. Interdiscip. Top.* **61,** 5149–5153.
43. Ravelli, F. & Antolini, R. (1992) *Biol. Cybern.* **67,** 57–65.
44. Govindan, R. B., Narayanan, K. & Gopinathan, M. S. (1998) *Chaos* **8,** 495–502.
45. Goldberger, A. L., Bhargava, V., West, B. J. & Mandell, A. J. (1986) *Physica D* (Amsterdam) **19,** 282–289.
46. Kaplan, D. T. & Cohen, R. J. (1990) *Circ. Res.* **67,** 886–892.
47. Jalife, J., Gray, R. A., Morley, G. E. & Davidenko, J. M. (1998) *Chaos* **8,** 79–93.
48. Karma, A. (1993) *Phys. Rev. Lett.* **71,** 1103–1106.
49. Karma, A. (1994) *Chaos* **4,** 461–472.
50. Winfree, A. T. (1994) *Science* **266,** 1003–1006.
51. Courtemanche, M. (1996) *Chaos* **6,** 579–600.
52. Panfilov, A. V. (1998) *Chaos* **8,** 57–64.
53. Qu, Z., Weiss, J. N. & Garfinkel, A. (1999) *Am. J. Physiol.* **276,** H269–H283.
54. Weiss, J. N., Garfinkel, A., Karagueuzian, H. S., Qu, Z. & Chen, P.-S. (1999) *Circulation* **99,** 2819–2826.
55. Qu, Z., Weiss, J. N. & Garfinkel, A. (2000) *Phys. Rev. E Stat. Phys. Plasmas Fluids Relat. Interdiscip. Top.* **61,** 727–732.
56. Qu, Z., Kil, J., Xie, F., Garfinkel, A. & Weiss, J. N. (2000) *Biophys. J.* **78,** 2761–2775.
57. Garfinkel, A., Chen, P.-S., Walter, D. O., Karagueuzian, H. S., Kogan, B., Evans, S. J., Karpoukhin, M., Hwang, C., Uchida, T., Gotoh, M., *et al.* (1997) *J. Clin. Invest.* **99,** 305–314.
58. Kim, Y.-H., Garfinkel, A., Ikeda, T., Wu, T.-J., Athill, C. A., Weiss, J. N., Karagueuzian, H. S. & Chen, P.-S. (1997) *J. Clin. Invest.* **100,** 2486–2500.
59. Zaitsev, A. V., Berenfeld, O., Mironov, S. F., Jalife, J. & Pertsov, A. M. (2000) *Circ. Res.* **86,** 408–417.
60. Damle, R. S., Kanaan, N. M., Robinson, N. S., Ge, Y. Z., Goldberger, J. J. & Kadish, A. H. (1992) *Circulation* **86,** 1547–1558.
61. Bayly, P. V., Johnson, E. E., Wolf, P. D., Greenside, H. S., Smith, W. M. & Ideker, R. E. (1993) *J. Cardiovasc. Electrophysiol.* **4,** 533–546.
62. Gray, R. A., Jalife, J., Panfilov, A. V., Baxter, W., Cabo, C., Davidenko, J. M. & Pertsov, A. M. (1995) *Science* **270,** 1222–1223.
63. Witkowski, F. X., Kavanagh, K. M., Penkoske, P. A., Plonsey, R., Spano, M. L., Ditto, W. L. & Kaplan, D. T. (1995) *Phys. Rev. Lett.* **75,** 1230–1233.
64. Hastings, H. M., Evans, S. J., Quan, W., Chong, M. L. & Nwasokwa, O. (1996) *Proc. Natl. Acad. Sci. USA* **93,** 10495–10499.
65. Witkowski, F. X., Leon, L. J., Penkoske, P. A., Giles, W. R., Spano, M. L., Ditto, W. L. & Winfree, A. T. (1998) *Nature (London)* **392,** 78–82.
66. Gray, R. A., Pertsov, A. M. & Jalife, J. (1998) *Nature (London)* **392,** 75–78.
67. Evans, S. J., Hastings, H. M., Nangia, S., Chin, J., Smolow, M., Nwasokwa, O. & Garfinkel, A. (1998) *Proc. R. Soc. London Ser. B* **265,** 2167–2170.
68. Bayly, P. V., KenKnight, B. H., Rogers, J. M., Johnson, E. E., Ideker, R. E. & Smith, W. M. (1998) *Chaos* **8,** 103–115.
69. Riccio, M. L., Koller, M. L. & Gilmour, R. F. (1999) *Circ. Res.* **84,** 955–963.
70. Small, M., Yu, D., Harrison, R. G., Robertson, C., Clegg, G., Holzer, M. & Sterz, F. (2000) *Chaos* **10,** 268–277.
71. Christini, D. J. & Collins, J. J. (1995) *Phys. Rev. E Stat. Phys. Plasmas Fluids Relat. Interdiscip. Top.* **52,** 5806–5809.
72. Smith, J. M., Clancy, E. A., Valeri, C. R., Ruskin, J. N. & Cohen, R. J. (1988) *Circulation* **77,** 110–121.
73. Konta, T., Ikeda, K., Yamaki, M., Nakamura, K., Honma, K., Kubota, I. & Yasui, S. (1990) *Circulation* **82,** 2185–2189.
74. Rosenbaum, D. S., Jackson, L. E., Smith, J. M., Garan, H., Ruskin, J. N. & Cohen, R. J. (1994) *N. Engl. J. Med.* **330,** 235–241.
75. Rosenbaum, D. S., Albrecht, P. & Cohen, R. J. (1996) *J. Cardiovasc. Electrophysiol.* **7,** 1095–1111.
76. Pastore, J. M., Girouard, S. D., Laurita, K. R., Akar, F. G. & Rosenbaum, D. S. (1999) *Circulation* **99,** 1385–1394.
77. Grill, S., Zykov, V. S. & Müller, S. C. (1995) *Phys. Rev. Lett.* **75,** 3368–3371.
78. Zykov, V. S., Mikhailov, A. S. & Müller, S. C. (1998) *Phys. Rev. Lett.* **78,** 3398–3401.
79. Osipov, G. V., Shulgin, B. V. & Collins, J. J. (1998) *Phys. Rev. E Stat. Phys. Plasmas Fluids Relat. Interdiscip. Top.* **58,** 6955–6958.
80. Osipov, G. V. & Collins, J. J. (1999) *Phys. Rev. E Stat. Phys. Plasmas Fluids Relat. Interdiscip. Top.* **60,** 54–57.
81. Rappel, W.-J., Fenton, F. & Karma, A. (1999) *Phys. Rev. Lett.* **83,** 456–459.